Supplementary Information

HMGA1 is a novel downstream nuclear target of the insulin receptor signaling pathway

Eusebio Chiefari, Maria T. Nevolo, Aurora Nocera, Stefania Iiritano, Elisa Maurizio, Riccardo Sgarra, Biagio Arcidiacono, Katiuscia Possidente, Camillo Palmieri, Francesco Paonessa, Giuseppe Brunetti, Guidalberto Manfioletti, Daniela Foti & Antonio Brunetti

Contents:

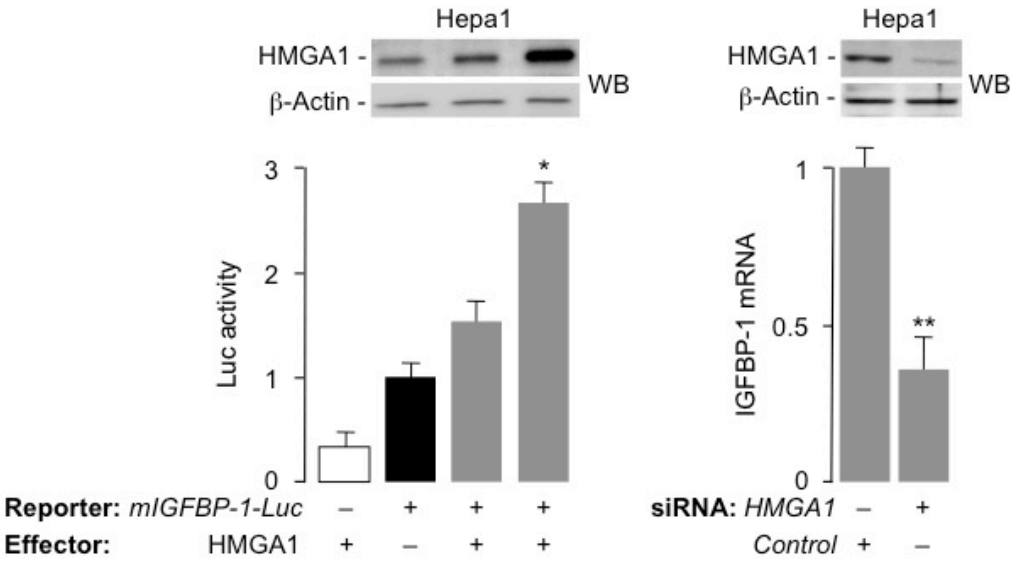

Supplementary Figure S1. Functional significance of HMGA1 for IGFBP-1 expression. Left, mouse *IGFBP-1*-Luc reporter vector (2 μg) was transfected into Hepa1 cells, plus increasing amounts (0, 0.5 or 1 μg) of *HMGA1* effector plasmid. Total plasmid DNA amounts were normalized with empty vector and Luc activity was assayed. Data represent the means ± s.e.m. for three separate experiments; values are expressed as factors by which induced activity increased above the level of Luc activity obtained in transfections with *IGFBP-1*-Luc reporter vector plus the empty effector vector, which is assigned an arbitrary value of 1. White bar, pGL3-basic vector (without an insert). Right, inhibition of endogenous IGFBP-1 mRNA in Hepa1 cells pretreated with anti-*HMGA1* siRNA or a nontargeting control siRNA. WBs of HMGA1 in each condition are shown in the autoradiograms. β-actin, control of protein loading. **P* < 0.05 versus control (black bar); ***P* < 0.05 versus siRNA-untreated (control) cells.

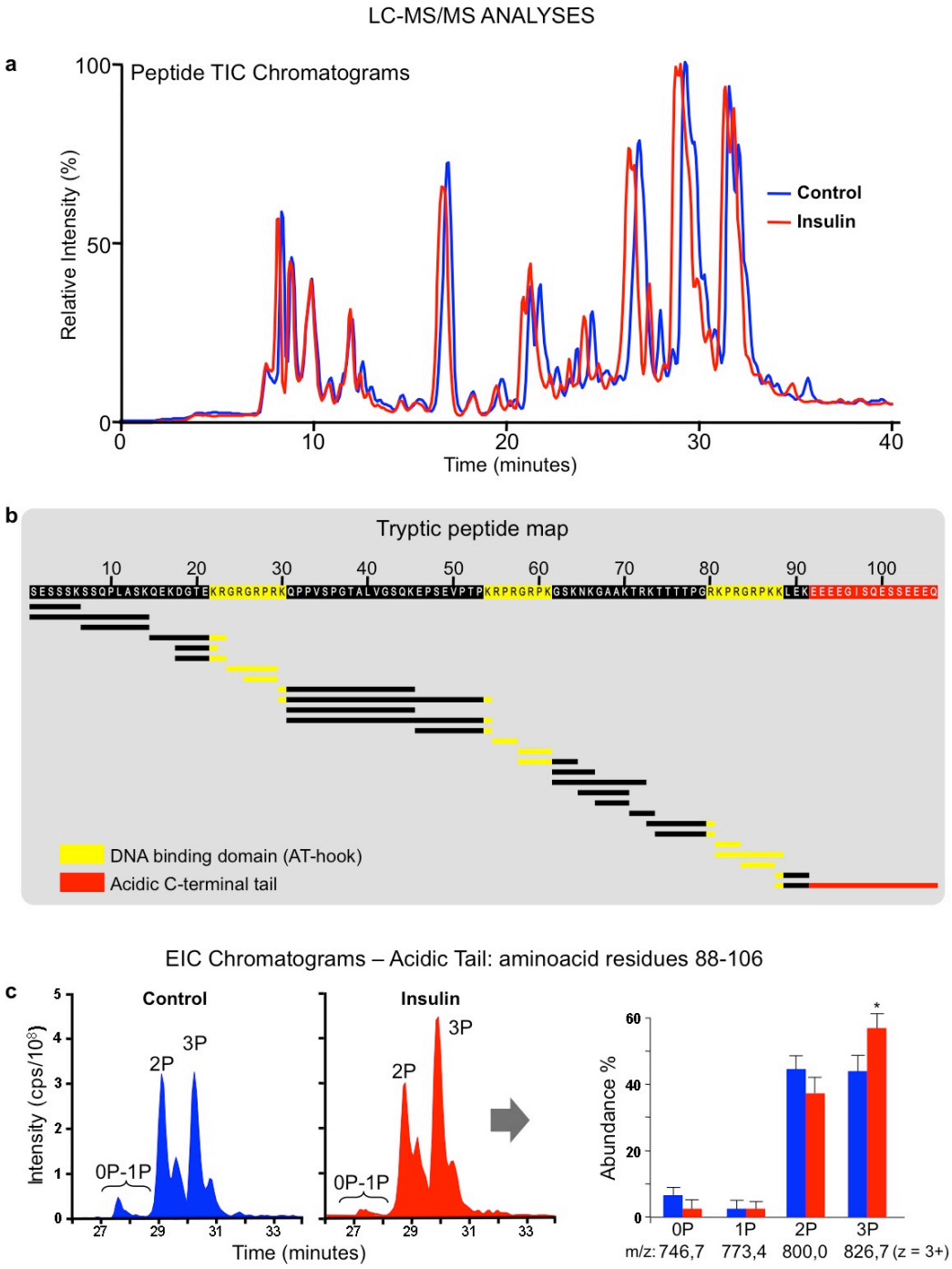

Supplementary Figure S2. Insulin-stimulated HMGA1a phosphorylation occurs predominantly at serine residues of the C-terminal peptide 88-106. HMGA1a was extracted from both untreated and insulin-treated HepG2 cells, purified by HPLC, and equal amounts of protein were trypsin digested and analysed by LC-MS/MS. (**a**) Total ion count (TIC) chromatograms of the HMGA1a tryptic peptides from control and insulin-treated HepG2 cells. (**b**) Sequence coverage of tryptic digests of the purified HMGA1a protein. Tryptic maps were generated by using the Mascot software (Matrix Sciences) and by manual inspection of LC-MS/MS analyses. (**c**) Extracted ion count (EIC) chromatograms of the various detected forms (0P-3P) of the C-terminal peptide 88-106, together with their percentage abundance (bar graphs). P, phosphorylation.

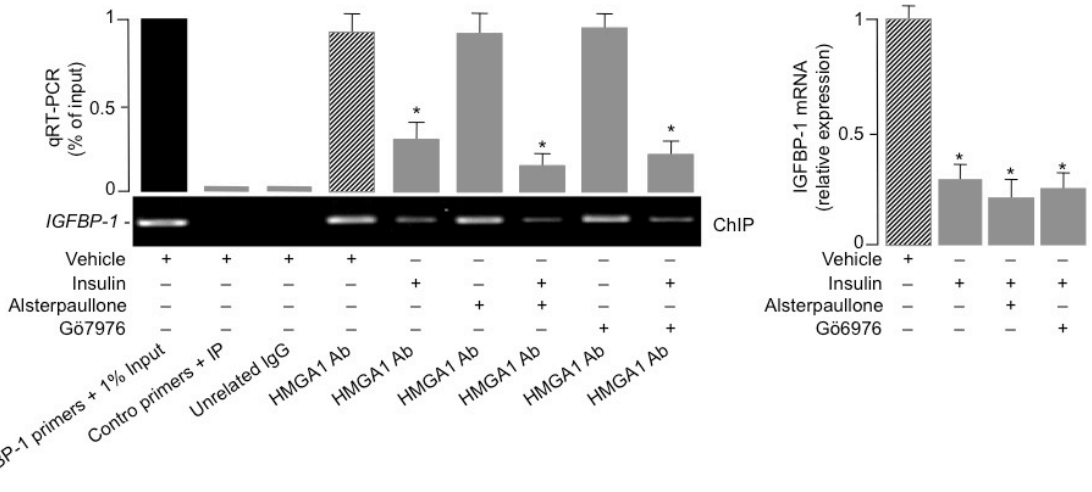

Supplementary Figure S3. Representative ChIP of *IGFBP-1* with anti-HMGA1 antibody (Ab) and qRT-PCR of ChIP-ed samples and endogenous IGFBP-1 mRNA (right side) in HepG2 cells untreated or treated with insulin, in the absence or presence of the cyclin-dependent kinase inhibitor alsterpaullone and the PKC inhibitor Gö6976. **P* < 0.05 versus untreated cells (slashed bars), in each assay.

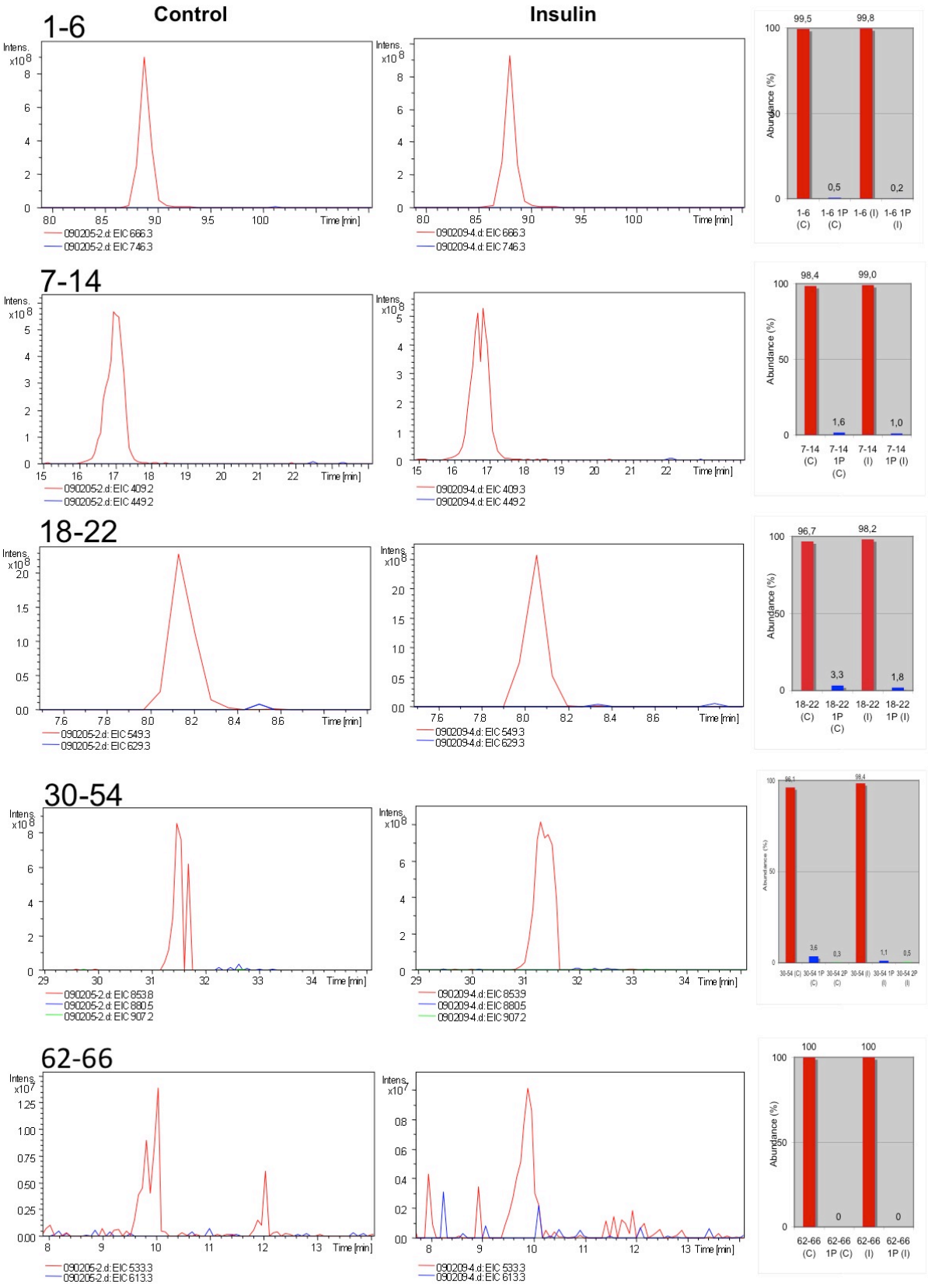
Control
Insulin
1-6
Intens.
x10 8
Time [min]
090205-2.d: EIC 666.3
090205-2.d: EIC 746.3
090209-4.d: EIC 666.3
090209-4.d: EIC 746.3
99,5
99,8
0,5
0,2
Abundance (%)
1-6 (C)
1-6 1P (C)
1-6 (I)
1-6 1P (I)
7-14
090205-2.d: EIC 409.2
090205-2.d: EIC 449.2
090209-4.d: EIC 409.3
090209-4.d: EIC 449.2
98,4
99,0
1,6
1,0
7-14 (C)
7-14 1P (C)
7-14 (I)
7-14 1P (I)
18-22
090205-2.d: EIC 549.3
090205-2.d: EIC 629.3
090209-4.d: EIC 549.3
090209-4.d: EIC 629.3
96,7
98,2
3,3
1,8
18-22 (C)
18-22 1P (C)
18-22 (I)
18-22 1P (I)
30-54
090205-2.d: EIC 853.8
090205-2.d: EIC 880.5
090205-2.d: EIC 907.2
090209-4.d: EIC 853.9
090209-4.d: EIC 880.5
090209-4.d: EIC 907.2
62-66
090205-2.d: EIC 533.3
090205-2.d: EIC 613.3
090209-4.d: EIC 533.3
090209-4.d: EIC 613.3
100
100
0
0
62-66 (C)
62-66 1P (C)
62-66 (I)
62-66 1P (I)

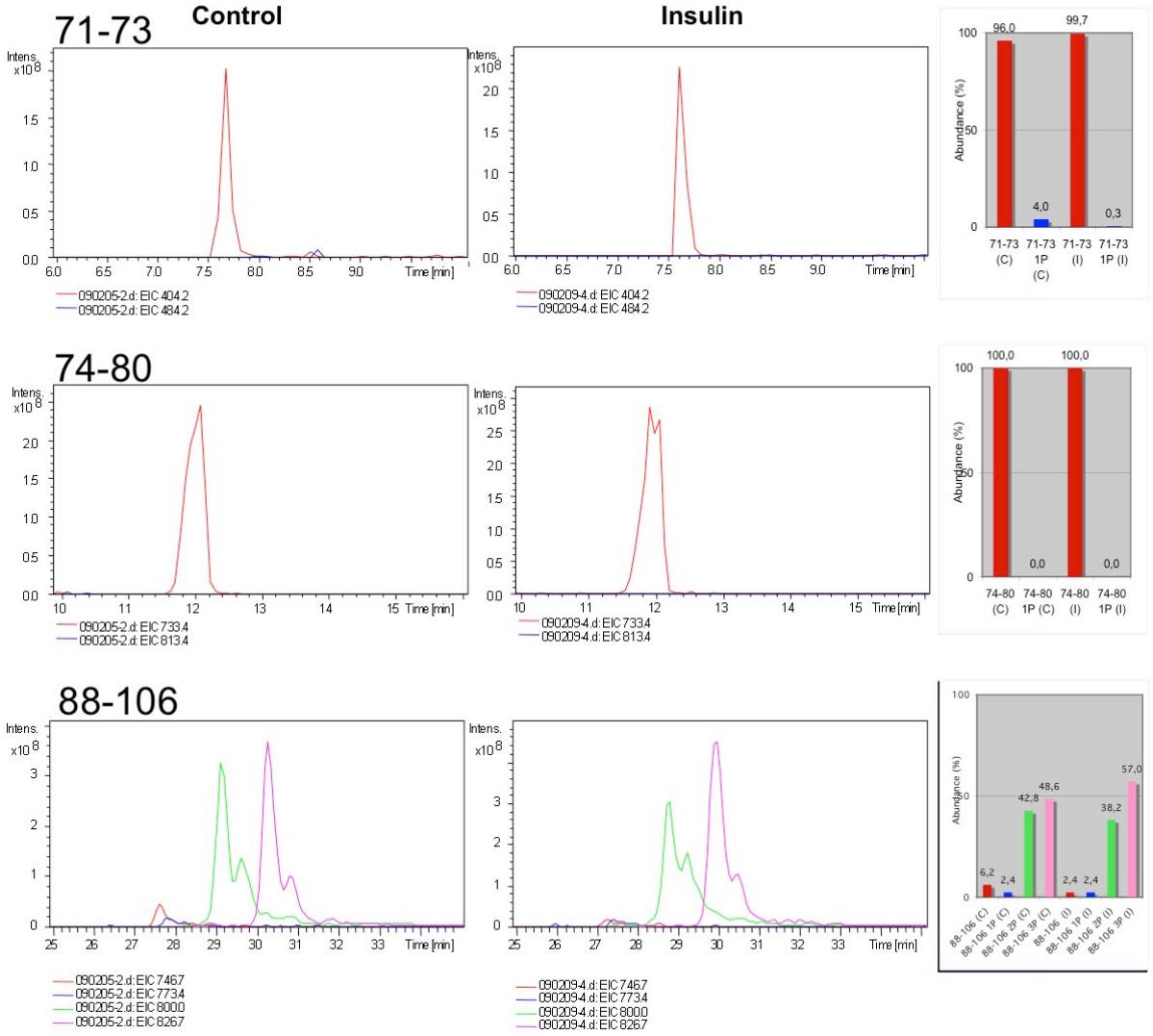

Supplementary Figure S4. Hyper-phosphorylation of HMGA1a during insulin response occurs on its C-terminal tail. LC-MS/MS analyses of HMGA1a protein extracted from control (C) and insulin-treated (I) cells have been inspected for the presence of phosphorylated peptides. TIC chromatograms of HMGA1a tryptic peptides ions are shown. Numbers reported in the upper-left corner indicate the aminoacid residues. Color code for lines and bars: red, unmodified peptide; blue, mono-phosphorylated peptide; green, bi-phosphorylated peptide; pink, three-phosphorylated peptide. Histogram graphs for peptide abundances (%) are reported on the right side of the figure.

peptide	RT	MM	m/z (1+)	cps (1+)			%
1-6 (C)	8,9	665,28	666,3	8,92E+08			99,5
1-6 1P (C)	10	745,28	746,3	4,08E+06			0,5
1-6 (I)	8,8	665,28	666,4	9,25E+08			99,8
1-6 1P (I)	8,6	745,28	746,3	1,62E+06			0,2
peptide	RT	MM	m/z (1+)	cps (1+)	m/z (2+)	cps (2+)	%
7-14 (C)	17	816,43	817,5	8,12E+08	409,2	5,65E+08	98,4
7-14 1P (C)	22	896,43	897,5	4,27E+05	449,2	9,43E+06	1,6
7-14 (I)	17	816,43	817,5	8,49E+08	409,3	5,23E+08	99,0
7-14 1P (I)	22	896,43	897	nd	449,2	5,46E+06	1,0
peptide	RT	MM	m/z (2+)	cps (2+)			%
15-23 (C)	15	1089,51	545,8	8,56E+06			93,9
15-23 1P (C)	15	1169,51	585,8	5,52E+05			6,1
15-23 (I)	15	1089,51	545,8	9,83E+06			98,4
15-23 1P (I)	15	1169,51	585,9	2,24E+05			2,2
peptide	RT	MM	m/z (1+)	cps (1+)			%
18-22 (C)	8,1	548,24	549,3	2,27E+08			96,7
18-22 1P (C)	9,5	628,24	629,3	7,76E+06			3,3
18-22 (I)	8,1	548,24	549,3	2,55E+08			98,2
18-22 1P (I)	9,8	628,24	629,3	4,78E+06			1,8
peptide	RT	MM	m/z (3+)	cps (3+)	m/z (4+)	cps (4+)	%
30-54 (C)	32	2557,37	853,8	8,51E+08	640,7	7,44E+08	96,1
30-54 1P (C)	33	2637,37	880,5	3,18E+07	660,6	5,67E+07	3,6
30-54 2P (C)	34	2717,37	907.2	2,37E+06	680,6	5,45E+06	0,3
30-54 (I)	31	2557,37	853,9	8,10E+08	640,7	7,37E+08	98,4
30-54 1P (I)	33	2637,37	880,5	8,76E+06	660,7	2,02E+07	1,1
30-54 2P (I)	33	2717,37	907.2	4,32E+06	680,6	3,61E+06	0,5
peptide	RT	MM	m/z (1+)	cps (1+)			%
62-66 (C)	18	532,29	533,4	1,61E+07			100
62-66 1P (C)	nd	612,99	nd	nd			nd
62-66 (I)	18	532,29	533,4	1,79E+07			100
62-66 1P (I)	nd	612,99	nd	nd			nd
peptide	RT	MM	m/z (1+)	cps (1+)			%
71-73 (C)	7,7	403,25	404,2	2,01E+08			96,0
71-73 1P (C)	8,6	483,25	484,2	8,40E+06			4,0
71-73 (I)	7,6	403,25	404,2	2,25E+08			99,7
71-73 1P (I)	8,5	483,25	484,2	7,50E+05			0,3
peptide	RT	MM	m/z (1+)	cps (1+)	m/z (2+)	cps (2+)	%
74-80 (C)	12	732,37	733,4	2,44E+08	367,2	8,65E+07	100,0
74-80 1P (C)	nd	812,37	813,4	nd	407,2	nd	nd
74-80 (I)	12	732,37	733,4	2,85E+08	367,2	5,76E+07	100,0
74-80 1P (I)	nd	812,37	813,4	nd	407,2	nd	nd
peptide	RT	MM	m/z (3+)	cps (3+)			%
88-106 (C)	28	2235,98	746,7	4,68E+07			6,2
88-106 1P (C)	28	2315,98	773,4	1,82E+07			2,4
88-106 2P (C)	29	2395,98	800	3,22E+08			42,8
88-106 3P (C)	30	2475,98	826,7	3,66E+08			48,6
88-106 (I)	27	2235,98	746,7	1,84E+07			2,4
88-106 1P (I)	27	2315,98	773,4	1,86E+07			2,4
88-106 2P (I)	29	2395,98	800	3,00E+08			38,2
88-106 3P (I)	30	2475,98	826,7	4,47E+08			57,0

Supplementary Table S1. Comparison of HMGA1a phosphorylated peptide abundances in control and insulin-treated cells. HMGA1a protein, extracted from control (C) and insulin (I) treated HepG2 cells, has been digested with trypsin and proteolytic peptides analysed by LC/MS. TIC for the various m/z signals corresponding to HMGA1a peptides have been obtained and a set of peptides covering all the serine/threonine residues of HMGA1a has been selected (reported in the first row). For each TIC the chromatographic retention time (RT) has been reported. The theoretical molecular masses of peptides (MM) are reported together with the observed m/z signals (with the indication of the charge state) and the intensity (cps) of the TIC peaks. The abundance of each peptide form (%) is reported. nd indicates that the m/z signal was not detected.

Supplementary Data. As shown by the tryptic map reported in Supplementary Fig. S2 we detected a set of tryptic peptides covering the entire HMGA1 sequence. From these peptides we selected the most abundant ones covering all serine/threonine residues embedded in HMGA1a sequence (aa: 1-6, 7-14, 15-23, 18-22, 30-54, 62-66, 71-73, 74-80, and 88-106). These peptides were detected both in control- and insulin-treated samples. For each of these peptides TIC were generated by extracting, from LC/MS data, the m/z signals corresponding to their unmodified, mono- (1P), bi- (2P), and tri-phosphorylated (3P) forms (Supplementary Fig. S4). Each TIC peak was manually inspected for the presence of the corresponding m/z value and charge state. Histogram graphs representing the percentage abundances of the various peptides have been generated on the basis of the data reported in Supplementary Table S1 and included in Supplementary Fig. S4 for easy quantitative interpretation of the data. As expected, other phosphorylated peptides were detected in addition to the C-terminal 88-106 peptide; however, it turned out that the phosphorylation level of these peptides was very low and that after insulin treatment there was a slight decrease in the abundance of these phosphorylated peptides. Taking peptide 7-14 as an example, it can be easily appreciated that the abundance of its mono-phosphorylated (1P) form decreases from 1.6% to 1% during insulin response. For these comparisons we selected ions having high and comparable intensities. The only peptide represented in Supplementary Fig. S4 having a lower intensity than the others is peptide 62-66. This is due to the fact that this is a peptide including a missed cleavage ($G_{62}S_{63}K_{64}N_{65}K_{66}$). Peptide $G_{62}SK_{64}$, which was probably the peptide most abundant in our tryptic digestion, is missing because its mass/charge value is under the lower limit of the range selected for LC/MS analyses. However, its phosphorylated counterpart has a m/z ratio above the lower limit of our range and we do not detect it in our LC/MS analyses. This, together with data of peptide 62-66, rules out the possibility that S_{63}, which is a PKC site, undergoes phosphorylation. Therefore, our data clearly assign hyper-phosphorylation of full length HMGA1a to its C-terminal domain.

Supplementary Video S1. Distribution of HMGA1 in HepG2 cells. Nuclear distribution of PAGFP-HMGA1a in living starved HepG2 cells, before and after 30-min treatment with either insulin alone, or insulin plus wortmannin. Consecutive confocal images were taken and assembled together in a time-lapse movie as the confocal plane progressed through the PAGFP-HMGA1a- or PAGFP-HMGA1am-expressing cell. Eleven image frames were taken over the course of 1 min 28 s.